J. Fluid Mech. (1987), *vol.* 184, *pp.* 551–569
Printed in Great Britain

An extension of the 'Malkus hypothesis' to the turbulent base flow of blunt sections

By WILLIAM S. VORUS AND LIYONG CHEN
Department of Naval Architecture and Marine Engineering, The University of Michigan, Ann Arbor, MI 48109-2145, USA

(Received 26 May 1986 and in revised form 20 April 1987)

This work develops and demonstrates an approximate theory for the mean turbulent near-wake of cylindrical bodies with blunt after edges. A closed free-streamline model is used to relate base pressure to the separation-streamline length. The additional relationship between base pressure and streamline length required for closure is an extension of the maximum dissipation hypothesis of Malkus, which was originally proposed for the turbulent-channel-flow problem. In the current application, the Malkus hypothesis leads to maximization of the rate of change of mean kinetic energy along the separation-cavity streamline.

The theory is implemented in terms of a linearized closed free-streamline theory of thin blunt-based symmetric sections, which was actually developed as an application to supercavitation, rather than separation. The calculations performed compare quite well with experimental measurements of mean base pressures and section drag. However, the linearizing assumptions on section-cavity slenderness and base-pressure magnitude are not so well preserved in the calculated results. Numerical analysis in terms of a nonlinear closed free-streamline model is a possible recourse. However, an important class of problems where the assumptions required in applying the linear theory may be better represented by the prevailing physics is the superseparation of thin lifting foils. This would appear to be the immediately most fruitful direction for the work, as a very mature theory of linearized supercavitation of thin lifting foils is available for providing the required free-streamline model.

Even though the formulation contains the effects of turbulent dissipation, the intricacies of the wake turbulence are avoided in achieving the solution. The lumped mean turbulent transfer rate per unit length of the mean dividing streamline is quantified, and defined in terms of the turbulence variables. Because of this, it is suggested that the theory may prove useful as a tool for studying wake turbulence characteristics.

1. Introduction

The subject of this paper is the high-Reynolds-number incompressible time-average turbulent flow behind two-dimensional shapes whose trailing edges are blunt, such that the separation-point positions are well defined (e.g. a wedge).

Experimentally, two-dimensional mean 'base flow' exhibits a closed cavity of relatively quiescent fluid separated from the largely ideal irrotational outer field by free shear layers. In the laminar case, below the critical Reynolds number prior to the appearance of vortex streets, the flow is essentially a steady pressure-driven flow characterized by two large symmetrical stationary eddies centred toward the rear of the separation cavity. Suitable theories have been proposed for this case (Smith 1985).

In the high-Reynolds-number turbulent case of interest here, the base flow is highly unsteady, being composed of a mean flow, onto which the shed boundary-layer turbulence and the coherent unsteadiness of the vortex streets are superimposed. Nevertheless, the experimental evidence is clear that, even in the midst of this chaotic unsteadiness, a mean streamline can be found which separates a basically stagnant interior flow, in the mean, from a basically ideal irrotational exterior mean flow (Russel 1958). The physics of the cavity closure are, however, very different from the steady subcritical laminar case. The turbulent base flow is Reynolds stress, rather than pressure, dominated. The closure results primarily from energy dissipation in the wake through nonlinear turbulence processes.

Anatol Roshko, in his famous paper (Roshko 1955), points out that the mean base pressure is intimately related to the mechanics of the wake turbulence, and that therein lies the key to a complete theory of turbulent base flow. Roshko also argues that either of the classic Kirchhoff or Raibouchinsky free-streamline models (Kirchhoff 1869; Raibouchinsky 1926) are valid elements of such a complete theory, but that an additional relationship between the wake turbulence and the mean base pressure is needed for system closure. Roshko then attempts to exploit a proposition of Heisenberg (1922) for coupling a modified Kirchhoff free-streamline model to Kármán's vortex-street model for the downstream wake. However, owing to uncertainties regarding the fraction of the total free-streamline vortex strength leaving the body which ultimately appears in the periodic street vortices downstream, Roshko's solution is not free of empiricism, requiring specific knowledge of the vortex shedding frequency for any particular case.

In the current proposition, the concept of the Raibouchinsky closed-streamline model is selected over the open-streamline model of Kirchhoff for providing the relationship between free-streamline geometry and base pressure. Following Kirchhoff, Raibouchinsky retained the assumption of uniform pressure within the separation cavity, but allowed for a lower cavity pressure by closing the free streamlines at some distance downstream of the separation points. Raibouchinsky's procedure, of course, does not define the cavity pressure and is therefore non-unique; the closed-streamline geometry is determinant only upon specification of the uniform cavity pressure. For the case of liquid supercavitation, where the uniform cavity gas pressure can be approximated as the known liquid vapour pressure, the basic Raibouchinsky concept is applied to this day. However, for 'superseparation', versus supercavitation, the base pressure is not obvious *a priori*. The additional relationship between cavity pressure and cavity geometry needed for uniqueness, which must necessarily involve the wake turbulence, has never appeared. Other than the remark of Roshko noting the general applicability to the turbulent-base-flow problem, the basic Raibouchinsky closed free-streamline concept does not appear to have been considered, until now, for application to other than liquid cavitation flows.

The classic theory of W. V. R. Malkus, which was specifically developed for the case of turbulent channel flow (Malkus 1956), is adapted here for providing the second relationship needed for closing a theory for turbulent base flow. The so-called 'Malkus hypothesis' is composed of a number of parts. The two parts most relevant to the current work are, stated concisely:

(i) the mean nonlinear momentum transport is entirely dissipative;

(ii) the dissipation rate is maximum.

These Malkus hypotheses are implemented with a closed free-streamline model of the separation cavity to achieve uniqueness in evaluating the mean base-flow

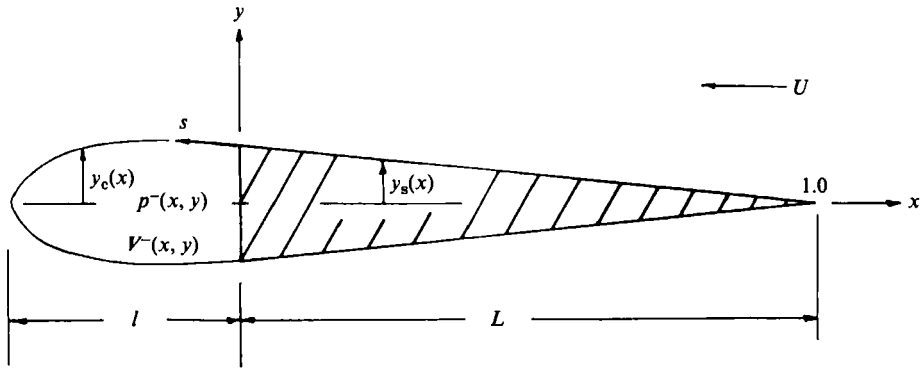

FIGURE 1. Section and cavity configuration.

characteristics of blunt sections. The implementation is accomplished by first lumping the mean wake vorticity as a vortex distribution along the separation streamline. This is an inherent requirement of the closed free-streamline model; the vortex strength is determined in terms of the unknown base pressure and the length of the mean streamline. The rate of change of vortex strength along the streamline is next related to the mean nonlinear turbulent transport by way of Helmholtz vorticity equation. The implied dissipation rate is then maximized, within the family of pressure–streamline length characteristics of the closed free-streamline model, to produce the required second relationship between base pressure and cavity length. The development details follow.

2. Turbulent dissipation

Consider the body to be of infinite span with a cylindrical section typical of the wedge depicted on figure 1. The cylinder is fixed in a uniform stream of velocity U in the negative x-direction as indicated.

The field velocity vector is generally a function of the three spatial coordinates as well as time, $\boldsymbol{V}(x, y, z, t)$. Ensemble average $\boldsymbol{V}$ in the z-direction over the infinite length of the cylinder. Assume $\boldsymbol{V}$ to be isotropic in z so that the spatial mean in z is also a temporal mean. Denote this mean velocity as $\boldsymbol{V}(x, y)$. With zero mean flow along the axis of the cylinder, $\boldsymbol{V}(x, y)$ is a two-component vector in cross-sectional planes.

Denote the variable component of $\boldsymbol{V}$ with zero mean in z and t as $\boldsymbol{V}_1(x, y, z, t)$ such that

$$\boldsymbol{V}(x, y, z, t) = \boldsymbol{V}(x, y) + \boldsymbol{V}_1(x, y, z, t). \tag{1}$$

Take the curl of (1) to produce the field vorticity vector as

$$\boldsymbol{\omega}(x, y, z, t) = \boldsymbol{\omega}(x, y) + \boldsymbol{\omega}_1(x, y, z, t). \tag{2}$$

Notice that $\boldsymbol{\omega}(x, y)$ in (2) is a single z-component vector due to the two-dimensionality of $\boldsymbol{V}(x, y)$ in (1).

The Helmholtz vorticity equation in three dimensions is

$$\rho \frac{\partial \boldsymbol{\omega}}{\partial t} - \rho(\boldsymbol{\omega} \cdot \boldsymbol{\nabla})\, \boldsymbol{V} + \rho(\boldsymbol{V} \cdot \boldsymbol{\nabla})\, \boldsymbol{\omega} = \mu \nabla^2 \boldsymbol{\omega}. \tag{3}$$

Focus attention on the z-component equation of (3), which exclusively involves the one-component mean vorticity vector $\omega(x, y)$, which is the unknown of direct interest. Substitute (1) and (2) into the z-component equation of (3), and apply the averaging operator to produce the following equation for the two-dimensional mean flow:

$$-\rho(\overline{\omega_1 \cdot \nabla V_{1z}}) + \rho(\overline{V_1 \cdot \nabla \omega_{1z}}) + \rho \nabla \cdot (V\omega) = \mu \nabla^2 \omega. \tag{4}$$

Here the overbar denotes a non-zero averaged result.

The mean nonlinear turbulence terms in (4) are the transfer to the turbulent dissipation scales, and according to the first of the Malkus hypotheses, the terms are entirely dissipative. They can be modelled as Reynolds stresses in terms of a turbulent diffusion, or dissipation, coefficient and incorporated with the molecular diffusion effect on the right-hand side of (4). If this is done the turbulent dissipation coefficient superimposes with the dynamic viscosity. Then, on elevating the Reynolds number Re to its assumed high level, the molecular diffusive effect becomes higher order relative to the turbulent dissipation, and can be discarded from the formulation.

Discard the molecular diffusion term in (4) as being higher order and denote the entire collection of turbulence terms as $\overline{R(x, y)}$. That is,

$$\overline{R(x, y)} + \rho \nabla \cdot (V\omega) = 0, \tag{5}$$

for Re very high.

It is now necessary to accept the existence of a mean dividing streamline traversing through the midst of the turbulent base flow. This streamline is viewed here as being approximately coincident with the midline of a mean turbulent shear layer which separates the outer ideal irrotational flow from the largely quiescent mean field within the separation cavity.

Referring to figure 2, denote by s the coordinate along the dividing streamline, positive downstream, with n normal, and lump the vorticity of the mean shear layer surrounding the streamline onto the streamline as

$$\omega(s, n) = \gamma(s)\, \delta(n). \tag{6}$$

Likewise write the mean field velocity in the streamline coordinates as

$$V(s, n) = V_s(s, n)\, \boldsymbol{e}_s + V_n(s, n)\, \boldsymbol{e}_n, \tag{7}$$

with the normal velocity on the streamline $V_n(s, 0) = 0$.

Substitute (6) and (7) into (5) and integrate the resulting equation in the n-direction across the shear layer to produce

$$\int_n \overline{R(s, n)}\, \mathrm{d}n + \rho \frac{\mathrm{d}}{\mathrm{d}s}(V_s \gamma) = 0. \tag{8}$$

Equation (8) applies along the separation streamline $n = 0$.

With the assumption of a stagnant flow inside the streamline, the vortex density, γ in (8), being equal to the velocity jump across the streamline, is just twice the streamline velocity, $V_s(s, 0)$. Replace γ by $2V_s(s, 0)$ in (8) and multiply the entire equation by $\frac{1}{4}$:

$$\frac{1}{4} \int_n \overline{R(s, n)}\, \mathrm{d}n = -\tfrac{1}{2} \rho \frac{\mathrm{d}}{\mathrm{d}s} V_s^2(s). \tag{9}$$

This is now an equation for the mean streamline velocity $V_s(s)$.

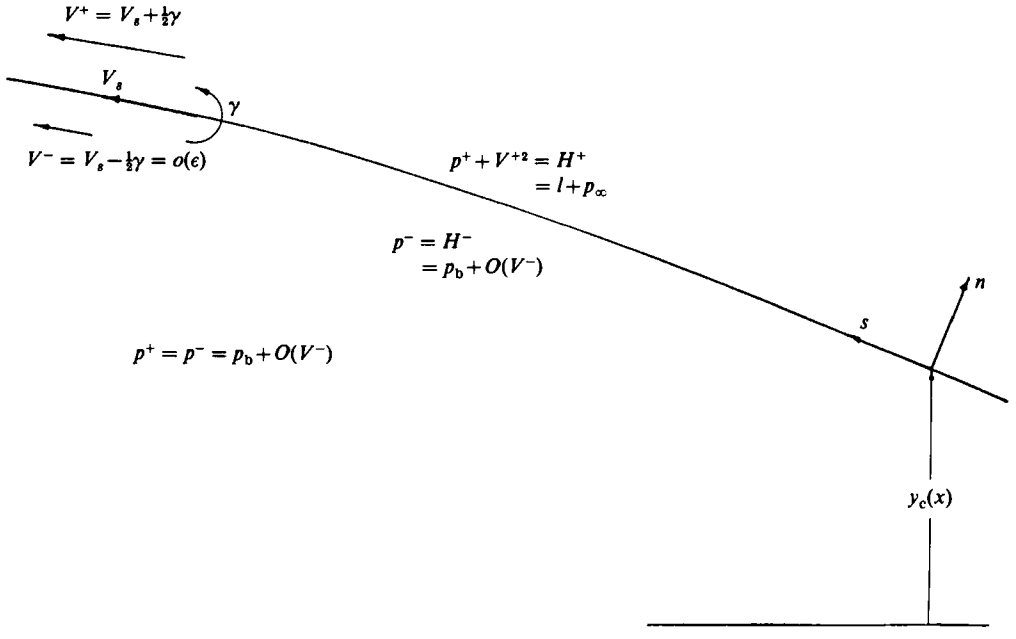

FIGURE 2. Conditions along the separation streamline.

The right-hand side of (9) is immediately recognized as the negative of the rate of change of mean kinetic energy per unit length of the dividing streamline, say $\mathscr{K}'(s)$. Redenote the collection of turbulence terms in (9) as $\mathscr{A}'(s)$. Equation (9) is then simply

$$\mathscr{A}'(s) = -\mathscr{K}'(s). \tag{10}$$

$\mathscr{A}'$ in (10) is identified as the rate of turbulent dissipation of mean kinetic energy per unit length of the streamline. The rate of change of kinetic energy density in (10) is negative, as the streamline velocity decreases with increasing s toward cavity closure downstream; this implies a positive dissipation rate, by (10), as is required.

By the second of the Malkus hypotheses, the dissipation rate is to be maximum. In constructing a dissipation functional to be maximized in seeking a closure relationship for the mean base flow, first integrate (10) in s:

$$\mathscr{A}(s) - \mathscr{A}(0) = \mathscr{K}(0) - \mathscr{K}(s). \tag{11}$$

$\mathscr{A}(s)$ is now the dissipation per unit length of the streamline. $s = 0$ corresponds to the body separation point and $s = l$ is the stagnation point at cavity closure. Take $\mathscr{A}(0) = 0$, since the bulk of the turbulent dissipation occurs after the onset of the global instability of the free shear layers and their degeneration into vortex streets, which is at some finite distance downstream of the separation points. Note from (11) that the dissipation per unit length (as well as its rate) will be maximum at streamline closure, $s = l$, where the kinetic energy density is zero. This is consistent with experimental evidence (Rouse 1961).

The total dissipation along the streamline $\mathscr{D}$ is obtained by integrating (11) over the length of the streamline:

$$\mathscr{D} = \tfrac{1}{2}\rho V_s^2(0)\, l - \tfrac{1}{2}\rho \int_{s=0}^{l} V_s^2(s)\, \mathrm{d}s. \tag{12}$$

Here the kinetic energy density has been rewritten in terms of the streamline velocity.

An *average rate* of dissipation over the length of the streamline $\mathscr{D}'$ is now obtained by dividing the total dissipation by the streamline length:

$$\mathscr{D}' = \frac{\mathscr{D}}{l} = \tfrac{1}{2}\rho V_s^2(0) - \tfrac{1}{2}\rho \frac{1}{l}\int_{s=0}^{l} V_s^2(s)\,\mathrm{d}s. \tag{13}$$

$\mathscr{D}'$ is the functional that will be maximized in implementing the Malkus hypothesis. $V_s(s)$ along the streamline in (13) can be written in terms of the base pressure, say P_b, and the streamline length by acknowledging conditions of streamline equilibrium. A second kinematical relationship between the base pressure and the streamline length, say $f(P_b, l) = 0$, is given by the closed free-streamline model for the separation cavity, as will be shown. $\mathscr{D}'$ is therefore a functional on P_b and l which is to be maximized subject to the equality constraint $f(P_b, l) = 0$. This is readily executed, in concept, to uniquely determine P_b and l for a given body geometry.

It can be observed from (13) that the dissipation functional is equivalent to the maximum kinetic energy density of the separated shear layer, which exists at the separation point, less its average value over the separation cavity length. It is important that this functional can be interpreted as approaching zero in both limits of long and short separation cavitites, utilizing the concepts of free-streamline theory.

The limiting long cavity is represented by the open Kirchhoff model in its near field. The entire turbulent dissipation might be viewed as occurring at the singular closure of this cavity at infinity, where the closure radius of curvature, relative to length, is zero. But the dissipation rate, by (13), over the infinite length of the Kirchhoff cavity is zero, as the constant free-streamline velocity gives an average kinetic energy density of the shear layer equal to its maximum value at separation.

The short-cavity limit, on the other hand, is the fully attached potential flow. Here, the average and maximum kinetic energy densities of (13) again cancel, but this time in singularities over the infinitesimally short cavities, as they collapse back into the separation points.

The existence of a non-zero, and in fact maximum, rate of dissipation of turbulent energy, by (13), between these two separation-streamline length extremes is essential to this work. But this is considered as implied by the prevailing logic.

3. Closed free-streamline model

Referring back to figure 1, the Navier–Stokes equations can be integrated inside the separation cavity to give

$$p^- + \boldsymbol{V}^- \cdot \boldsymbol{V}^- = H^-(x, y). \tag{14}$$

All variables are now expressed non-dimensionally, with the non-dimensionalization on the section length L, the stream speed U, and the water density ρ. Pressures and forces are relative to the dynamic head $\frac{1}{2}\rho U^2$. $H^-(x, y)$ in (14) is the 'total head' inside the separation cavity, which varies in an unspecified way with position within the cavity.

Assume that the fluid velocity inside the cavity is small, relative to a small parameter ϵ; ϵ should in some way be related to Reynolds number, decreasing as the Reynolds number increases. $\boldsymbol{V}^- = o(\epsilon)$, such that to $O(\epsilon)$, from (14),

$$p^-(x, y) = H^-(x, y) + o(\epsilon).$$

Further, write

$$p^-(x,y) = p^-(0,0)+[p^-(x,y)-p^-(0,0)]. \tag{15}$$

Define the first term in (15) as the 'base pressure', p_b, and assume it to be $O(1)$. Assume the difference between the base pressure and the cavity interior field pressure in (15) to be $O(V^-)$. The relative cavity pressure is then, to lowest order,

$$P_b = p_b - p_\infty. \tag{16}$$

With p_∞ representing the static pressure of the uniform stream, P_b is the base pressure coefficient, by the usual definition.

It is very convenient at this point to assume that both p_b and p_∞ are $O(1)$, but that their difference, P_b, is ϵ order. If this is done, and the section and attached cavity are furthermore together assumed to be slender, with the slenderness parameter taken as ϵ, then the generally nonlinear closed free-streamline theory reduces to the linear theory of steady two-dimensional supercavitation (Tulin 1953, 1955). It is only necessary that the cavitation number appearing in that theory be replaced by $-P_b$. For the sake of completeness, the required free-streamline solution by way of the linearized supercavitating theory is outlined as follows.

3.1. *Linearized theory*

First restrict the geometry to symmetric (non-lifting) sections. This is in the interest of simplicity of the demonstration; the linearized procedure applies similarly to the lifting case. Following specifically the presentation of Newman (1977), the linearized kinematic boundary conditions, to $O(\epsilon)$, applied on the section and cavity axes, respectively, are (refer to figure 1):

$$v(x,0) = -y_s'(x) \quad \text{on} \quad 0 \leqslant x < 1, \tag{17}$$

$$v(x,0) = -y_c'(x) \quad \text{on} \quad -l < x < 0. \tag{18}$$

$v(x,y)$ is the perturbation velocity component in the vertical direction.

An additional boundary condition, a dynamic condition, is required on the cavity boundary, since its position is unknown *a priori*. This condition is continuity of pressure across the cavity streamline. Referring to figure 2, the requirement $p^+ = p^-$ across the streamline gives

$$p_\infty - p_b = V^{+2} - 1. \tag{19}$$

But $p_\infty - p_b \equiv -P_b$, by (16), which is $O(\epsilon)$ by the linearizing assumption.

The velocity on the outer edge of the streamline, V^+, to $O(\epsilon)$ is,

$$V^+ = 1 - u(x,0), \tag{20}$$

where $u(x,y)$ is the axial perturbation velocity. Substitution of (20) into (19) gives the required dynamic boundary condition, to $O(\epsilon)$, on the cavity axis:

$$u(x,0) = \tfrac{1}{2}P_b \quad -l < x < 0. \tag{21}$$

3.2. *Solution*

The Hilbert problem represented by (17) and (21) is solved for a source distribution on the cavity axis as a function of P_b; it is, on $-l < x < 0$:

$$q(x) = P_b\left(\frac{-x}{l+x}\right)^{\frac{1}{2}} - \frac{2}{\pi}\left(\frac{-x}{l+x}\right)^{\frac{1}{2}} \int_{t=0}^{1} \left(\frac{l+t}{t}\right)^{\frac{1}{2}} \frac{y_s'(t)}{t-x}\,\mathrm{d}t. \tag{22}$$

The remaining cavity kinematic boundary condition, (18), is then used to evaluate the locus of the cavity contour as

$$y_c(x) = y_s(0) + \frac{1}{2}\int_{\xi=0}^{x} q(\xi)\,\mathrm{d}\xi. \tag{23}$$

The cavity length is determined in terms of P_b by acknowledging cavity closure as $y_c(-l) = 0$ in (23). There results, utilizing (22),

$$P_b - \frac{4}{\pi l}\int_{t=0}^{1}\left(\frac{l+t}{t}\right)^{\frac{1}{2}} y_s'(t)\,\mathrm{d}t = 0. \tag{24}$$

The pressure drag (coefficient) per unit span is then finally available as

$$D = \frac{1}{\pi l y_s(0)}\left[\int_{x=0}^{1} y_s'(x)\frac{l+2x}{[x(l+x)]^{\frac{1}{2}}}\,\mathrm{d}x\right]^2, \tag{25}$$

where the non-dimensionalization involves the section base depth, $2y_s(0)$.

Formula (24) above is the relationship denoted as $f(P_b, l) = 0$ in the discussion following (13); it is the second relationship between cavity base pressure and length required to close the mean base-flow solution. Formulas (19) and (20) also give the streamline velocity required in the dissipation maximization at (13). Non-dimensionally, to order ϵ

$$V_s(s) = \tfrac{1}{2}(1 - \tfrac{1}{2}P_b). \tag{26}$$

However, it is first necessary to recognize that (26) is not uniformly valid over the cavity streamline. Thin-body theory, in general, is, in fact, not uniformly valid to any order, without special correction. Specifically, solutions are invalid at the body ends; the assumptions made on orders of magnitude in achieving the thin-body perturbation expansion are violated at the ends, in general. This is readily apparent in the current problem. By (26), the cavity streamline velocity is constant over the streamline length. But the velocity along the contour cannot be constant if the cavity closes, and it must be zero at the after stagnation point. The dilemma is here easily eliminated to produce a uniformly valid first-order representation of V_s, which exhibits the correct behaviour at the separation cavity end, by the well-known procedure of M. J. Lighthill (1951).

3.3. *Lighthill correction of surface flow*

The Lighthill correction (Lighthill 1951) is produced by a purely kinematical local coordinate stretching. It removes the divergent characteristics of the thin-body perturbation expansion which first appears at the body ends in the third order, and renders the expansion valid at the ends and uniformly convergent to the first two orders. Actually, Lighthill developed the correction for the leading-edge flow of aerofoils with camber and incidence as well as thickness, but it can be interpreted for trailing edges as well. The only requirement is that the thin-body edge, or end, possess a well-defined radius of curvature.

Lighthill proceeds to show that the applicable coordinate stretching involves no more than a local shift of the existing end singularity to a point on the axis one-half the radius of curvature inside the body end.

In the case at hand, which involves the end of the separation cavity, which is the

thin body after end, the required coordinate shift is effected by modifying the contour streamline velocity, (26), as

$$V_s(s) = \tfrac{1}{2}(1-\tfrac{1}{2}P_b)\left[\frac{l-s}{l-s+\frac{1}{2}\rho_{TE}}\right]^{\frac{1}{2}}. \tag{27}$$

Here ρ_{TE} is the cavity trailing edge radius of curvature. Normally, ρ_{TE} would be fixed by the specified body geometry. In the present case it is expressible in terms of the problem unknowns, P_b and l, by definition, as

$$\lim_{s\to l} y_c(s) = [2\rho_{TE}(l-s)]^{\frac{1}{2}},$$

or, differentiating,

$$\lim_{s\to l} y_c'(s) = \left[\frac{\rho_{TE}}{2(l-s)}\right]^{\frac{1}{2}}. \tag{28}$$

Then, with $q(s) = 2y_c'(s)$ from (23),

$$\rho_{TE}(P_b, l) = \tfrac{1}{2}\lim_{s\to l}[(l-s)^{\frac{1}{2}}q(s)]^2. \tag{29}$$

$q(s)$ is available from (22), with x replaced by $-s$ for convenience.

It is obvious that the corrected surface velocity, (27), possesses the correct behaviour with regard to cavity closure. At the stagnation point, $s = l$, the velocity is zero, as required. On the other hand, for $\rho_{TE}/l = o(1)$, the velocity deviates only slightly from its constant uncorrected value, (26), until entering the immediate vicinity of the stagnation point. The smaller ρ_{TE}, the more concentrated the effect. Obviously, the Lighthill correction allows axial derivatives to be first order at the body ends, which is the fallacy of the uncorrected theory.

It is convenient to re-note here, in connection with (27), that the turbulent dissipation, as defined by (8)–(12), are all identically zero for the Kirchhoff open free-streamline model. In that model, the vortex density along the open free streamline, and hence the free-streamline velocity, is constant. The vortex density is equal to the uniform stream speed and the streamline velocity is half the stream speed; this is necessary for the requirement of that model that the base pressure within the open cavity should equal the free-stream static pressure. This is entirely consistent with the recognized physics. Kinematically, the free streamlines can close only if the vortex density decreases along the streamlines (Ribaut 1983). The vortex density decreases along the streamlines owing to turbulent dissipation, which results in the mean closed cavity found in turbulent base flows. The Kirchhoff open model must therefore be viewed as the ideal asymptotic model in the limit of zero turbulent dissipation. The alternative interpretation cited earlier as that of an infinitely long cavity closed with non-zero turbulent dissipation at infinity does not satisfy the maximum dissipation requirement of (13).

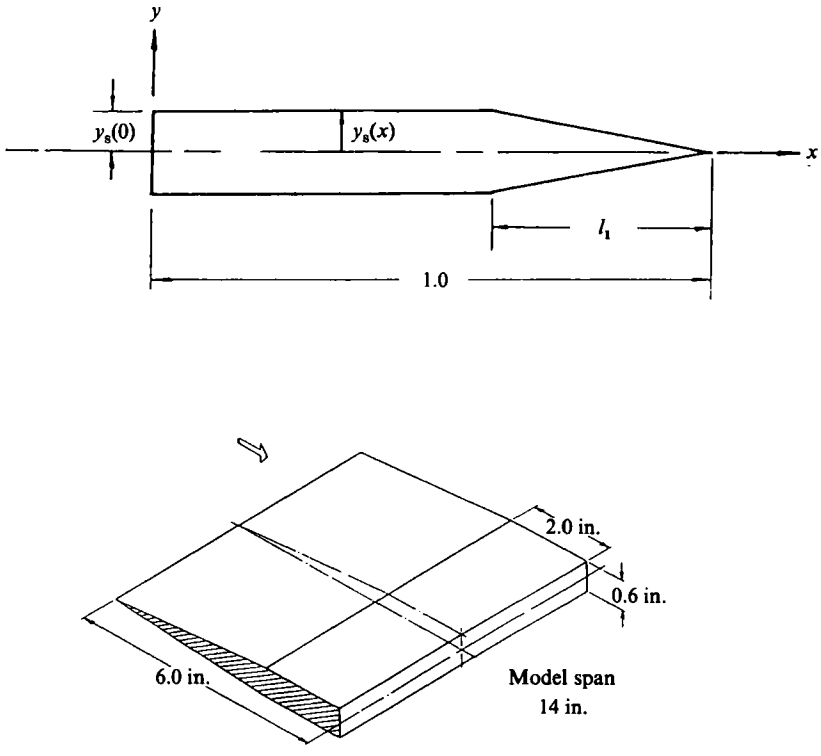

FIGURE 3. Nash form.

4. Solutions and applications

Substituting (27) into (12), the non-dimensional average turbulent dissipation rate is

$$\mathscr{D}' = \tfrac{1}{4}(1-P_b)\left[\frac{1}{1+\alpha} - \int_{\zeta=0}^{1} \frac{1-\zeta}{1-\zeta+\alpha}\,\mathrm{d}\zeta\right], \tag{30}$$

where $\alpha = \frac{1}{2}\rho_{TE}/l$, with ρ_{TE} given in terms of P_b and l by (29) and (22). The integration in (30) is readily performed to produce, to lowest order,

$$\mathscr{D}' = -\tfrac{1}{4}(1-P_b)\,\alpha(1+\ln\alpha). \tag{31}$$

Here α has been assumed to be $O(\epsilon)$, as is required by the Lighthill theory. Then one relation between P_b and l is obtained as

$$\mathscr{D}'(P_b, l) = \max. \tag{32}$$

The other, referred to in the preceding section as $f(P_b, l) = 0$, is (24).

Upon specification of the section geometry, $y_s(x)$, (32) and (24), with (29) and (22), determine the first-order base pressure and separation cavity length. Equation (25) then gives the section base drag.

4.1. *Nash form*

Figure 3 depicts the blunt-trailing-edge section used in the base flow experiments of J. F. Nash (Nash, Quincey & Callinan 1963). The specific dimensions of the

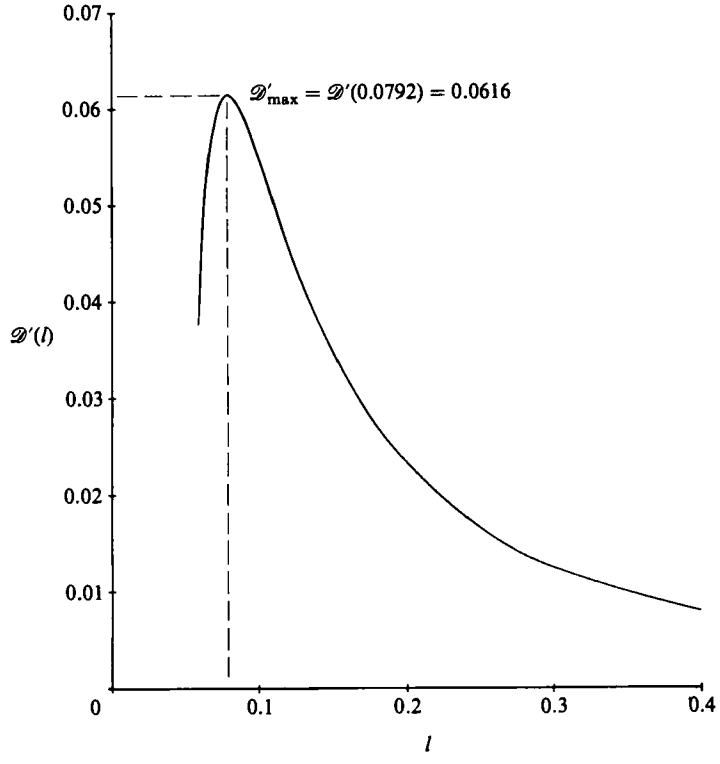

FIGURE 4. Dissipation rate versus separation cavity length, Nash form.

configuration tested in the high-speed wind tunnel at NPL are indicated on the figure. This section type is somewhat general in that it includes the wedge section for $l_1 = 1$, and at the other extreme, it becomes the semi-infinite parallel-sided section as $y_s(0)$ and l_1 tend to zero.

The section geometric input required in the preceding formulas is exclusively the contour slope distribution, $y'_s(x)$. For the figure 3 section,

$$y'_s(x) = \begin{cases} -y_s(0)/l_1 & 1-l_1 < x \leqslant 1, \\ 0 & 0 < x \leqslant 1-l_1. \end{cases} \tag{33}$$

Substitute (33) into (24), (25) and (29), and then define

$$A(l, l_1) \equiv (l+1)^{\frac{1}{2}} - [(1+l-l_1)(1-l_1)]^{\frac{1}{2}}. \tag{34}$$

The solution formulation reduces to (31):

$$\mathscr{D}' = -\tfrac{1}{4}(1-P_b)\alpha(1+\ln\alpha)$$

with

$$\alpha = \left[\frac{4y_s(0)}{\pi l}\frac{A(l,l_1)}{2l_1}\right]^2, \tag{35}$$

which is to be maximized, subject to

$$P_b + \frac{4y_s(0)}{\pi l l_1}\left\{A(l,l_1) + l\ln\left[\frac{(1+l)^{\frac{1}{2}}+1}{(1+l-l_1)^{\frac{1}{2}}+(1-l_1)^{\frac{1}{2}}}\right]\right\} = 0. \tag{36}$$

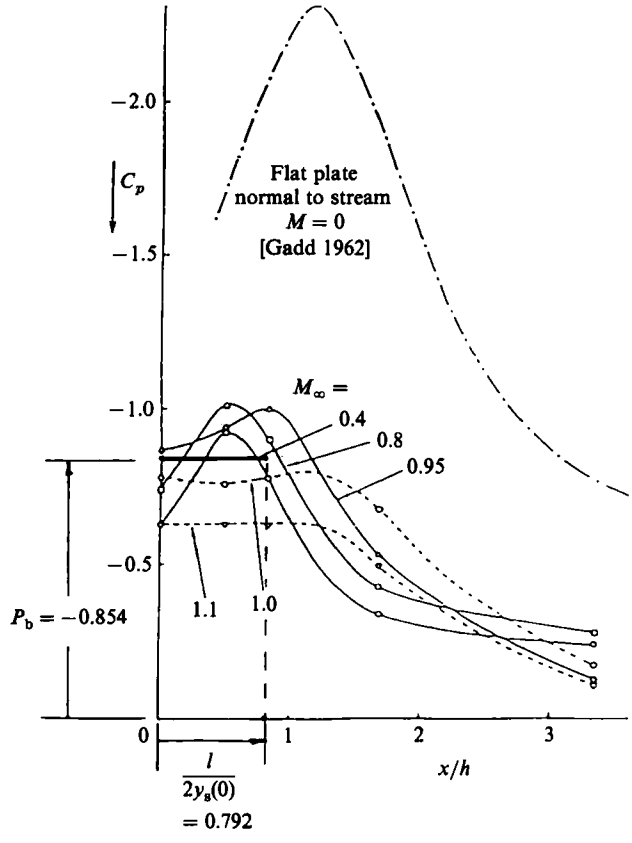

FIGURE 5. Nash form base-pressure variation.

Then, the base drag coefficient per unit span is

$$D = \frac{4y_s(0)}{\pi l}\left[\frac{A(l, l_1)}{l_1}\right]^2. \tag{37}$$

Figure 4 is a plot of $\mathscr{D}'(l)$ for the Nash form with $y_s(0) = 0.05$ and $l_1 = 0.6667$, which was the configuration tested (figure 3). P_b has been eliminated in $\mathscr{D}'$ of the figure 4 plot by substitution of (36) directly into (31). The solution point at $l = 0.0792$ is clearly evident on figure 4. The base pressure coefficient corresponding to this cavity length is calculated from (36) as $P_b = -0.854$. The maximum non-dimensional turbulent energy transfer rate at the solution point is $\mathscr{D}'_{max} = 0.0626$, from figure 4.

A selection of Nash's experimental base-pressure results are shown on figure 5. This is a plot of mean pressure coefficient versus non-dimensional distance along the centreline of the wake, for varying Mach number M. The Reynolds number at the lowest Mach number of 0.4 was approximately 1.5×10^6.

The calculated mean separation-cavity characteristics corresponding to the uniform first-order base pressure of $P_b = -0.854$ at the cavity length to base depth ratio of 0.792 are indicated on figure 5.

Perhaps the most immediately notable aspect of the comparison on figure 5 is the character of the measured wake centreline pressure versus the calculated first-order base pressure over the cavity length. Nash warns that the experimental wake

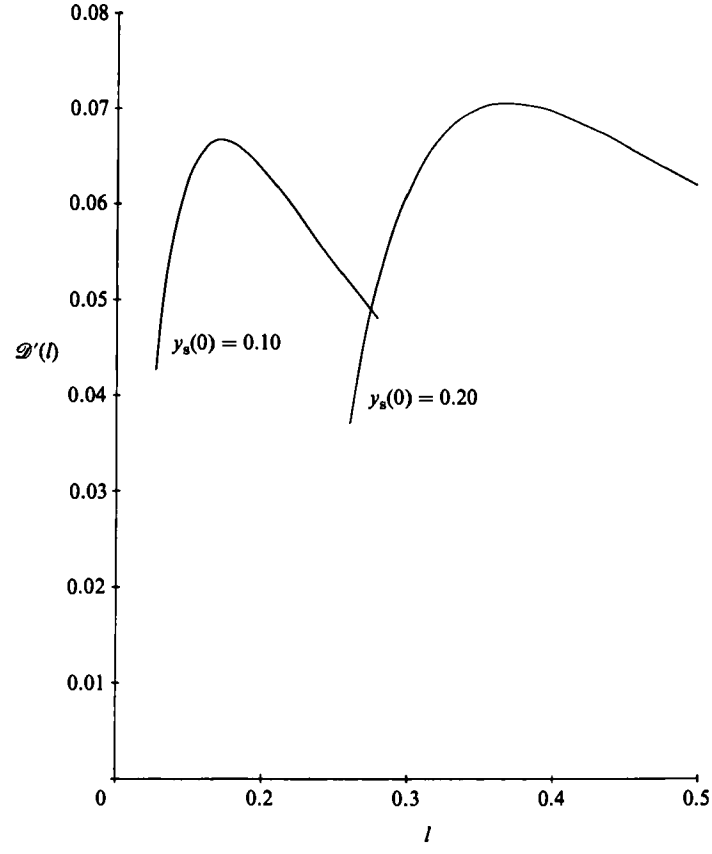

FIGURE 6. Dissipation rate versus separation cavity length, 10 and 20% wedges.

pressures of figure 5 were difficult to measure and are of questionable accuracy. Nevertheless, with due respect for this reservation, the measured data at the Mach number of 0.4, which is the only one of the set of much relevance here, suggests that the mean flow within the cavity still has some significant spatial variability at the test Reynolds number of approximately 1.5×10^6; this spatial variability, in the mean, has been assumed to be higher order in the calculation, by (15). The negative pressure peak at approximately one-half the base depth downstream is thought to be due to the destabilization of the separated shear layers and their degeneration into vortex streets (Nash *et al.* 1963). It has been postulated (Goldstein 1938) that with increasing Reynolds number the vortex streets give way to more-or-less random turbulence. Furthermore, with the shear layers tending to destabilize and breakdown into turbulence closer to the body with increasing Re, it is tempting to conjecture that the limiting state, at very high Re, is an intensely chaotic, but, more-or-less randomly distributed turbulent flow, whose temporal mean, within the separation cavity, is basically quiescent. For such a flow, the mean pressure within the separation cavity would be expected to be more-or-less uniform, and not characterized by the pronounced peak exhibited in the Nash data. Any experimental evidence that suggests that the subject pressure peak flattens at very high Reynolds number (and at low Mach number) has, however, not been uncovered.

Of course, the pressure must rise on approaching cavity closure, and far enough

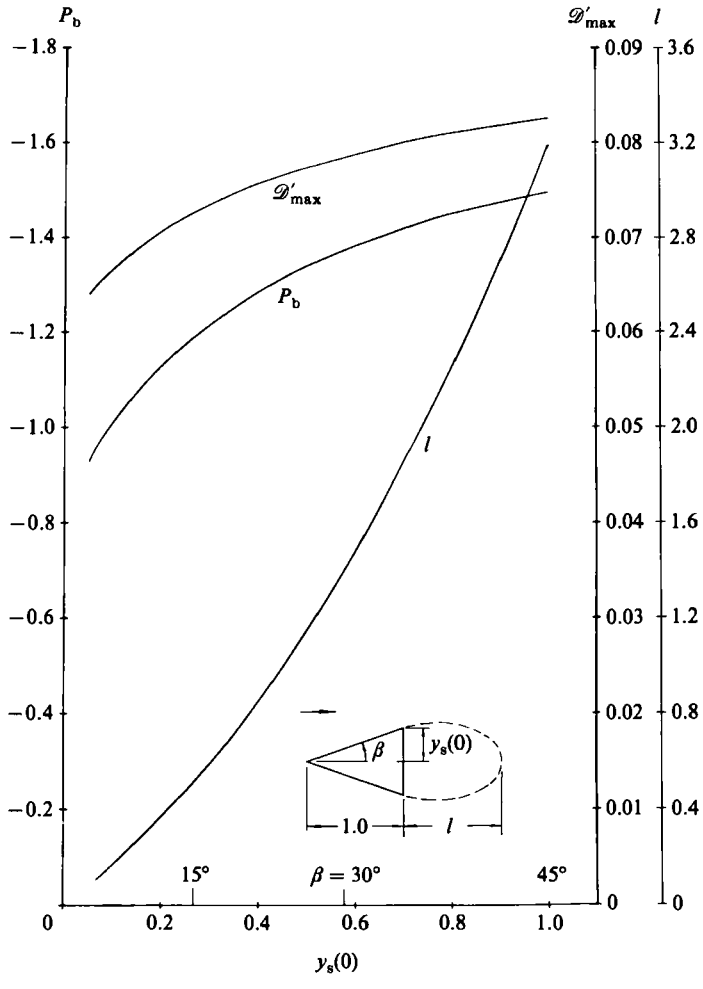

FIGURE 7. Base-pressure coefficient, cavity length, and maximum dissipation rate versus wedge base offset.

downstream it must return to the free-stream static pressure. This trend is obvious in the Nash data of figure 5. The Lighthill correction could easily be applied to the uniform first-order base pressure to imply the rising characteristic downstream along the mean streamline. However, the predicted total head recovery at streamline closure so obtained would be erroneous. The concept employed here of lumping the mean field vorticity onto the separation streamline may be acceptable for purposes of approximating an integrated average dissipation rate, with the integral being reasonably tolerant to deviance very near the closure point. However, the pressure details at mean streamline closure are certainly not within the limits of the approximation. An average base pressure, reasonably representative away from cavity closure, such as that depicted on figure 5, is probably about as much as can be expected from the proposed theory.

4.2. *Semi-infinite parallel-sided section*

Observe from figure 3 that if the length of the parallel after-section of the Nash form, $0 \leqslant x \leqslant 1-l_1$, tends to infinity, the dimensions $y_s(0)$ and l_1, which are non-dimensional on the section length, tend to zero. The cavity length l, which should in this case be of the order of $y_s(0)$, should then also tend to zero. Assuming l and l_1 to be of the same small order, $A(l, l_1)$, by (34), becomes, to lowest order, $A(l, l_1) = l_1$. Then, (35), (36) and (37) become, to lowest order,

$$\alpha = \frac{1}{4}\left[\frac{4y_s(0)}{\pi l}\right]^2, \quad P_b + \frac{4y_s(0)}{\pi l} = 0, \quad D = -P_b.$$

Equation (31) is unaltered. The solution for this case therefore depends only on the ratio $y_s(0)/l$, and is therefore independent of scale, as it must be. The solution is

$$\frac{y_s(0)}{l} = 0.633, \quad P_b = -0.806, \quad \mathscr{D}'_{max} = 0.0600.$$

Note that this does not represent the solution for the rearward-facing step. In that case, $y = 0$ downstream of separation must be interpreted as a rigid plane. The presence of such a plane prevents the development of vortex streets, and thereby suppresses the large-scale turbulent mixing and the associated mean energy transfer to the dissipation scales. The rearward-facing-step problem, or any base-flow problem with a rigid plane of symmetry, appears to be more like the pressure-driven laminar base flow, where the internal cavity dynamics play the dominant role. The base pressures are much higher (less negative) and the mean cavity lengths much longer there than in the Reynolds-stress-dominated base flow treated in this work (Nash *et al.* 1963; Arie & Rouse 1956).

4.3. *Wedge*

If l_1 is set to unity in (34)–(37), the Nash form (figure 3) becomes a wedge. In this case, with $A(l, l_1) = (1+l)^{\frac{1}{2}}$, the relevant formulas are $\mathscr{D}'$, by (31), which remains unchanged, and the following:

$$\alpha = \frac{1}{4}\left[\frac{4y_s(0)}{\pi l}\right]^2 (1+l), \tag{38}$$

$$P_b + \frac{4y_s(0)}{\pi l}\left[(1+l)^{\frac{1}{2}} + l \ln \frac{1+(1+l)^{\frac{1}{2}}}{l^{\frac{1}{2}}}\right] = 0, \tag{39}$$

$$D = \frac{4y_s(0)}{\pi l}(1+l). \tag{40}$$

Similar to figure 4, figure 6 is a plot of $\mathscr{D}'(l)$, from (31), (38) and (39), for wedge bases of 10 and 20%. The solution points, at $l = 0.171$ and 0.370, respectively, are clearly evident on figure 6.

Figure 7 is a plot of wedge base-pressure coefficient P_b, separation cavity length l, and the maximum dissipation rate $\mathscr{D}'_{max}$, versus wedge base offset.

The drag coefficient versus $y_s(0)$ is plotted on figure 8. The experimental data points indicated are from the experiments of Lindsey (1938).

Lindsey's drag experiments were conducted in an 11 in. high-speed wind tunnel

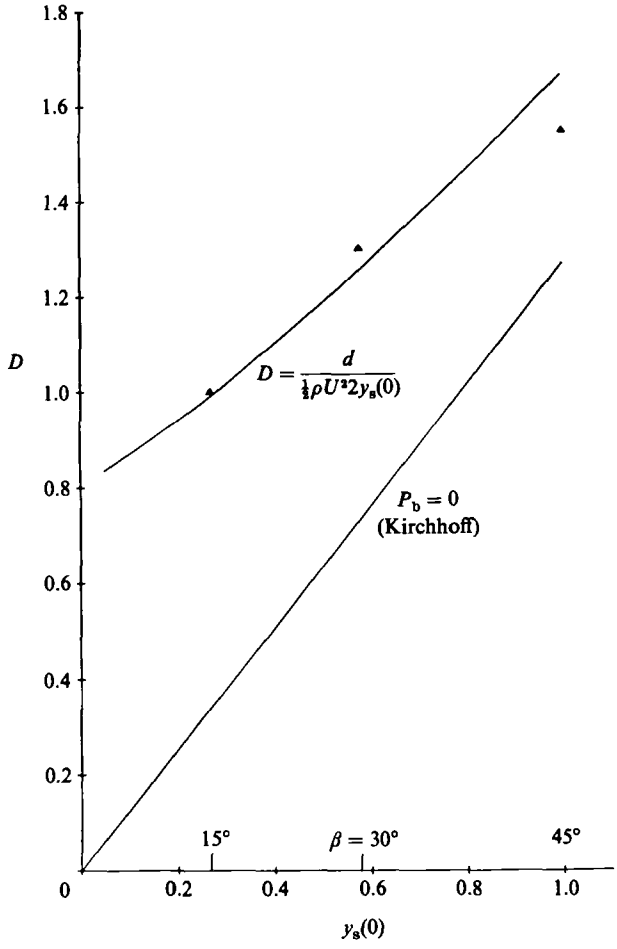

FIGURE 8. Drag coefficient versus wedge base offset; ▲, data from Lindsey (1938).

using a pendulum-type force balance. The experimental drag coefficients shown for the 15°, 30°, and 45° half-angle wedges were tested at Reynolds numbers of 10^5, 4×10^4, 2×10^4, respectively, but at a common Mach number of approximately 0.35. The wedges all had the same base depth $y_s(0)$, but different lengths to achieve the different apex angles.

Lindsey's complete data set shows a very mild variation in drag coefficient with Reynolds number in the test range of approximately 2×10^3–10^5. This indicates that the drag forces were dominated by pressure, rather than skin-friction effects, and should therefore be validly comparable to the theoretical predictions of figure 8, which include no skin-friction drag at all. The theory requires a high but unspecified Reynolds number.

The drag coefficient corresponding to Kirchhoff's open free-streamline model with $P_b = 0$ is included on figure 8 for reference; the Kirchhoff drag coefficient for the wedge is simply

$$D = \frac{4y_s(0)}{\pi}.$$

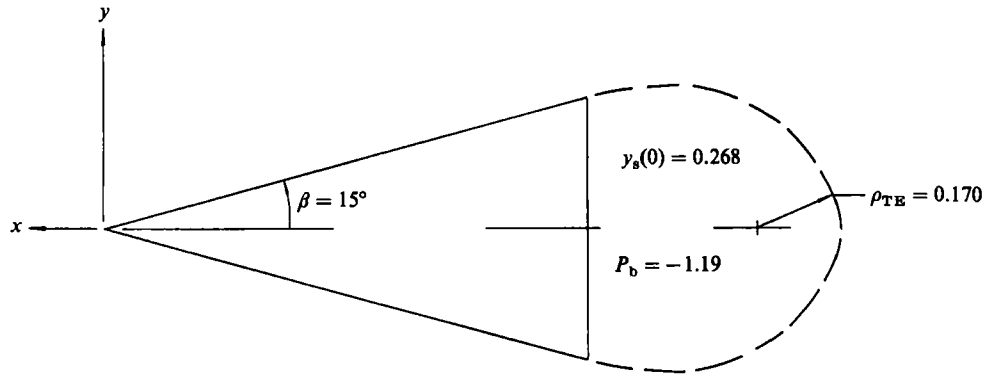

FIGURE 9. Wedge and separation cavity, half-apex angle = 15°.

4.4. *Discussion*

While the preceding results are undeniably encouraging with regard to the applicability of the proposed theory, it is in order to re-examine the assumptions implemented in the light of the some of the predicted magnitudes.

Most critically, the section and attached separation cavity were assumed to be slender, and base pressure was assumed to be of slenderness order. These assumptions were necessary for allowing the convenience of simple linearized cavity flow theory for the closed free-streamline model. However, from the ensuing analysis and calculations based on this assumption, the predicted base pressure is clearly of order of the free-stream dynamic head, which is $O(1)$. The minimum absolute value, for the semi-infinite parallel sided-section, is $|P_b| = 0.806$, and values well in excess of 1.0 are predicted for the wedges (figure 8). This implies axial perturbation velocities of around half that of the free stream, from (21).

Further to this, figure 9 is a plot of the 15° ($y_s(0) = 0.268$) wedge section and its calculated cavity streamline. This body would not be described as particularly thin; thinness is the basis of the linearized theory (a correction, the Lighthill correction, was, however, made for the relative bluntness of the cavity end). The parameter α for the figure 9 case, corresponding to $\rho_{TE} = 0.170$ and $l = 0.522$ is $\alpha = 0.163$; α was specifically assumed to be $o(1)$ in achieving the $\mathscr{D}'$ formula for the linearized theory, (31).

5. Conclusion

The stretching of the theoretical assumptions that has exposed itself in the calculations is troublesome, as it arouses the suspicion that the good results could be fortuitous. The uncertainties arise entirely from the use of linearized cavity flow theory for the closed free-streamline model. That very simple and convenient theory is linearized on the basis of the thinness of the section and its attached separation cavity, as well as on the basis of a small cavity (base) pressure coefficient. The resulting cavity lengths and pressure coefficients calculated on the basis of the linearizing assumptions, while comparing very favourably with experimental results on mean turbulent base flow, are nevertheless not inarguably of the magnitudes assumed. It was actually recognized beforehand that the correct magnitude of the base pressure associated with blunt-body separation was not clearly in accord with the assumptions of the linearized theory. Nevertheless, linearized theory was applied

in view of its convenience. What was not anticipated was that the resulting predictions would be so correct!

Any uncertainty is, of course, resolved by implementing the theory with a nonlinear closed free-streamline model, e.g. Ribaut (1983). In spite of the order-of-magnitude increase in numerical complexity required to produce numbers for comparison with experiment, the procedure should be reasonably straightforward. The requirement, basically, would be to find a closed cavity streamline contour that satisfied the kinematic boundary condition of zero normal velocity, and to find a variable vortex strength along that contour such that the average dissipation rate, by (13), was maximum. Such a procedure would require several layers of iteration, or, perhaps preferably, would be implemented by a mathematical programming technique as a constrained optimization problem. Of course, the insight provided by application of the more approximate linear theory exhibited here would be totally obliterated.

The linearized formulation demonstrated here should however be more applicable to a different, but probably more important, class of problems: that is, back separation of streamlined lifting sections rather than base separation of blunt symmetric sections. The pressure perturbations are typically smaller with separated lifting sections. A stalling foil, with separation points at the leading and trailing edges, experimentally demonstrates suction-side pressures more on the order consistent with the assumptions of the linearized theory. The linearized theory of super-cavitation of lifting foils is well developed, and conveniently available for extending the theory to lifting problems.

A final note concerns the usefulness of the theory, in the event that such is ultimately established. This is perhaps in the study of base-flow turbulence itself. On solution for the mean separation streamline velocity, a prediction of the turbulent dissipation rate per unit length of the streamline, $\mathscr{d}'(s)$, is given by (10). It is interesting to contemplate the experimental construction of $\mathscr{d}'(s)$ in terms of the measured turbulent quantities defined by (9), and comparison with the theoretically deduced function.

REFERENCES

Gadd, G. E. 1962 Two-dimensional Separated or Cavitating Flow Past a Flat Plate Normal to the Stream. *Aero. Res. Counc. Conf. Proc.* 697, November.

Goldstein, S. 1938 *Modern Developments in Fluid Dynamics*, Vol. II, pp. 553–554, 557–559. Clarendon.

Arie, M. & Rouse, H. 1956 Experiments on two-dimensional flow over a normal wall. *J. Fluid Mech.* **1**, 129–141.

Heisenberg, W. 1922 Die Absoluten Dimensionen der Karmanschen Wirbelbewegung. *Phys. Z.* **23**, 363.

Kirchhoff, G. 1869 Zur Theorie Freier Flussigkeitsstrahlen. *Krelles J.* **70**, 289–298.

Lighthill, M. 1951 A new approach to thin aorifoil theory. *Aero. Q.* **III**, November.

Lindsey, W. 1938 Drag of cylinders of simple shapes. *NACA Tech. Rep.* 619.

Malkus, W. V. R. 1956 Outline of a theory of turbulent shear flow. *J. Fluid. Mech.* **1**, 521–539.

Nash, J. F., Quincey, V. G. & Callinan, J. 1963 Experiments on two-dimensional base flow at subsonic and transonic speeds. *Aero. Res. Counc. R & M* 3427, January.

Newman, J. 1977 *Marine Hydrodynamics*. MIT Press.

Raibouchinsky, D. 1926 On some cases of two-dimensional fluid motion. *Proc. Lond. Math Soc.* **25**, 185–194.

Ribaut, M. 1983 A vortex sheet method for calculating separated two-dimensional flows. *AIAA J.* August.

ROSHKO, A. 1955 On the wake and drag of bluff bodies. *J. Aero. Sci.* **17**, 124–132.

ROUSE, H. 1961 Energy transformation in zones of separation. In *Proc. Ninth Intl Assoc. for Hyd. Res., Dubrovnik.*

RUSSEL, A. 1958 Aerodynamics of wakes, existence of unsteady cavities. *Engineering* **186**, 701–702.

SMITH, F. T. 1985 A structure for laminar flow past a bluff body at high Reynolds number. *J. Fluid Mech.* **155**, 175–191.

TULIN, M. 1953 Steady two-dimensional cavity flows about slender bodies. *David Taylor Model Basin Rep.* 834, Washington, D.C.

TULIN, M. 1955 Supercavitating flow past foils and struts. In *Proc. Symp. on Cavitation in Hydrodyn. Natl. Phys. Lab., London.*